Cell Reports
Physical Science

CellPress
OPEN ACCESS

Article

Anchoring single platinum atoms onto nickel nanoparticles affords highly selective catalysts for lignin conversion

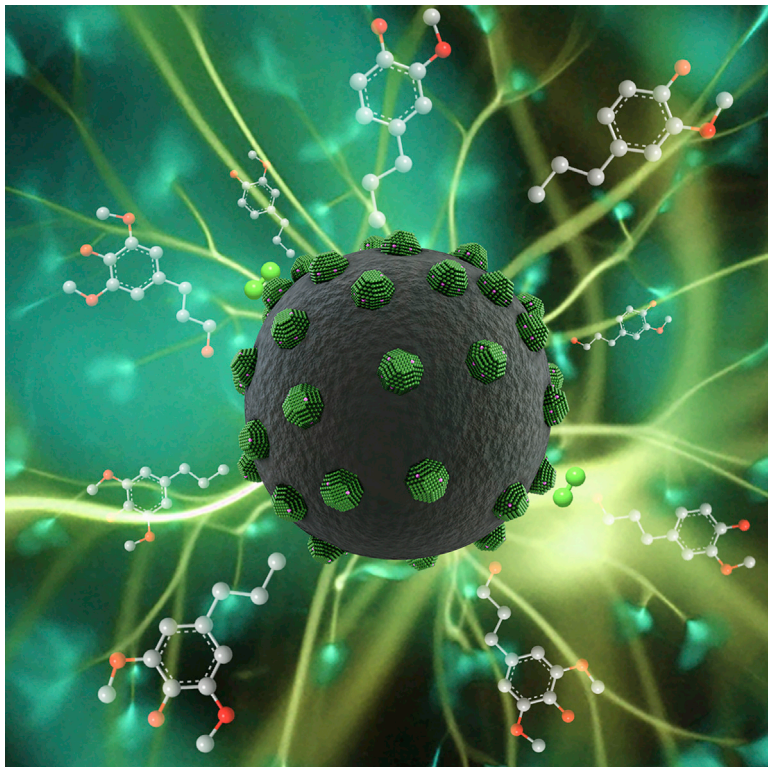

Alloying noble metal atoms with non-noble metals allows the atomic efficiency of the noble metal to be maximized. Chen et al. describe single-atom catalysts for reductive lignin depolymerization based on platinum single atoms anchored onto nickel nanoparticles and supported on carbon, which are highly efficient, with the structure of the catalysts determining the selectivity of the reaction.

Lu Chen, Linfeng Pan, Antoine P. van Muyden, ..., Anders Hagfeldt, Gabor Laurenczy, Paul J. Dyson

gabor.laurenczy@epfl.ch (G.L.)
paul.dyson@epfl.ch (P.J.D.)

Highlights

An efficient single-atom alloy catalyst for lignin-first biorefining is disclosed

The catalyst shows high activity in lignin deconstruction to afford aromatic monomers

Key structural and mechanistic features of the catalyst are provided

Chen et al., Cell Reports Physical Science *2*, 100567
September 22, 2021
https://doi.org/10.1016/j.xcrp.2021.100567

Cell Reports
Physical Science

CellPress
OPEN ACCESS

Article

Anchoring single platinum atoms onto nickel nanoparticles affords highly selective catalysts for lignin conversion

Lu Chen,[1] Linfeng Pan,[1,2] Antoine P. van Muyden,[1] Lichen Bai,[3] Jun Li,[4] Yun Tong,[1,5] Zhaofu Fei,[1] Anders Hagfeldt,[2,6] Gabor Laurenczy,[1,*] and Paul J. Dyson[1,7,*]

SUMMARY

Due to the highly complex polyphenolic structure of lignin, depolymerization without a prior chemical treatment is challenging, and new catalysts are required. Atomically dispersed catalysts are able to maximize the atomic efficiency of noble metals, simultaneously providing an alternative strategy to tune the activity and selectivity by alloying with other abundant metal supports. Here, we report a highly active and selective catalyst comprising monodispersed (single) Pt atoms on Ni nanoparticles supported on carbon (denoted as Pt_1Ni/C, where Pt_1 represents single Pt atoms), designed for the reductive depolymerization of lignin. Selectivity toward 4-n-propylsyringol and 4-n-propylguaiacol exceeds 90%. The activity and selectivity of the Pt_1Ni/C catalyst in the reductive depolymerization of lignin may be attributed to synergistic effects between the Ni nanoparticles and the single Pt atoms.

INTRODUCTION

Lignin is an abundant biomass source that can be converted into value-added aromatic platform chemicals.[1] To use biomass to its fullest, the challenges involved in valorizing lignin need to be overcome.[2–5] Conventional lignocellulose delignification methods, such as Kraft and organosolv pulping, require the complete breakdown of the C–O bonds in a series of steps.[6–8] However, the ability to deconstruct lignin directly from raw biomass has transformed the conventional concept of the biorefinery by capturing high-value products from lignin in the first step,[9] a process that is particularly effective under reductive conditions.[3,10–12] The lignin is depolymerized and selectively converted to monomers with high retention of carbohydrates in the pulp.[10,13,14] The monomers obtained are valuable platform chemicals with a range of applications. Further use of the remaining cellulose and hemicellulose provides additional value-added chemicals.[15–17]

Using noble metal catalysts (e.g., Rh, Ru, Pd, Pt), the yields of lignin monomers can reach close to the theoretical maximum.[18–20] However, these noble metal catalysts are expensive and can be susceptible to poisoning by CO or coking.[21] Efforts to maximize the efficiency of these noble metal catalysts with improved selectivity has led to the development of atomically dispersed heterogeneous catalysts.[22–24] All of the reaction steps take place at single-atom sites and, compared with metal nanoparticles (NPs), the reaction kinetics with single-atom catalysts are rate limited by the low concentration of H atoms available in the active atomic sites.

Progress toward catalyst design to combine the activity of noble metals and low cost of earth-abundant metals is popular.[25] Some earth-abundant metals such as Ni have

[1]Laboratory of Organometallic and Medicinal Chemistry, Institute of Chemical Sciences and Engineering, Ecole Polytechnique Federale de Lausanne (EPFL), 1015 Lausanne, Switzerland

[2]Laboratory of Photomolecular Science, Institute of Chemical Sciences and Engineering, EPFL, 1015 Lausanne, Switzerland

[3]Laboratory of Inorganic Synthesis and Catalysis, Institute of Chemical Sciences and Engineering, EPFL, 1015 Lausanne, Switzerland

[4]Laboratory of Photonics and Interfaces, Institute of Chemical Sciences and Engineering, EPFL, 1015 Lausanne, Switzerland

[5]Department of Chemistry, School of Sciences, Zhejiang Sci-Tech University, 928 Second Avenue, Xiasha High Education Zone, Hangzhou 310018, P.R. China

[6]Department of Chemistry – Ångström Laboratory, Uppsala University, 75120 Uppsala, Sweden

[7]Lead contact

*Correspondence: gabor.laurenczy@epfl.ch (G.L.), paul.dyson@epfl.ch (P.J.D.)

https://doi.org/10.1016/j.xcrp.2021.100567

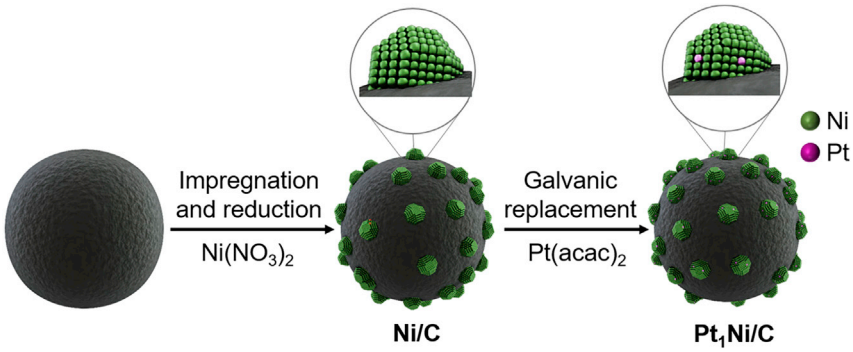

Scheme 1. Route used to prepare the Pt_1Ni/C catalyst

low energy barriers for both the dissociation of H_2 and the diffusion of H atoms.[26] If H_2 dissociation on Ni NPs and diffusion to active single noble metal atoms is facile, then the rate-limiting addition of H atoms to the substrate should be accelerated, improving the overall reaction kinetics and reducing the amount of the precious metal required. Such a single-atom alloy (SAA) concept has been described for a PdCu system in which facile hydrogen dissociation and spillover take place.[27] Because the dissociation of H_2 and reaction sites on SAAs are decoupled, SAAs may not be confined to linear scaling relationships, exceeding the reactivity limit and selectivity of many catalysts.

Despite numerous reports of SAAs, their application is mostly limited to catalytic process involving small substrates and in reactions such as C-C coupling, hydrogenation, and electrocatalytic processes.[22,28–33] There are only limited studies describing SAAs as catalysts for biomass transformations, with the focus on lignin model compounds as substrates.[34,35] Direct depolymerization of lignin using SAAs has not, to the best of our knowledge, been reported.

Here, we describe a highly active catalyst for reductive lignin depolymerization based on Pt single atoms anchored onto Ni NPs supported on C (denoted as Pt_1Ni/C, where Pt_1 represents single Pt atoms). Using this catalyst, a yield of lignin monomers of 37% for birch sawdust was achieved under 5 MPa H_2 in methanol (MeOH) at 200°C, which is significantly higher than that using single Pt atoms supported on active carbon Pt_1/C or Ni NPs on active carbon Ni/C.

RESULTS

Catalyst synthesis and characterization

The Pt_1Ni/C catalyst was obtained by anchoring Pt atoms on Ni NPs supported on C (Ni/C) through galvanic replacement (Scheme 1). In the synthesis, $Pt(acac)_2$ dissolved in toluene was added to a suspension of Ni/C in ethanol. C was chosen as the support as it is inexpensive and has a high surface area and cavities where H_2 can be adsorbed.[36] Following washing with ethanol and hexane, the Pt_1Ni/C catalyst was obtained as a black powder. Inductively coupled plasma-atomic emission spectroscopy (ICP-AES) analysis of the Pt_1Ni/C catalyst gives weight percentages of the Pt and Ni as 0.3 and 4.4 wt%, respectively. Thermogravimetric analysis (TGA) of Pt_1Ni/C in air (Figure S4) confirmed that the loading of metal NPs is ~5%. The specific surface area of Pt_1Ni/C is 90.4 m^2/g (Figure S5). Using transmission electron microscopy (TEM), the diameter of the Ni NPs was found to be ~6.9 nm with a narrow size distribution (Figure S1), a size that is similar to Ni/C (Figure S7).

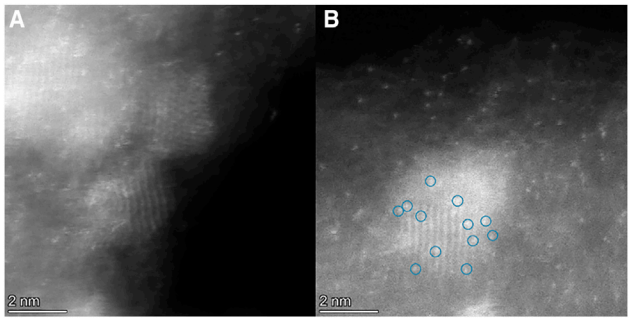

Figure 1. HAADF-STEM images

(A) HAADF-STEM image of the Pt_1Ni/C catalyst.

(B) HAADF-STEM image of an individual Pt_1Ni nanoparticle. The monodispersed Pt atoms are highlighted in blue circles and are uniformly anchored on the surface of Ni NPs.

The distribution of Pt on Ni/C within the Pt_1Ni/C matrix was analyzed by high-angle annular dark-field scanning TEM (HAADF-STEM) (Figure 1), which confirms that the Pt atoms are highly dispersed (the isolated Pt atoms are manifested by brightness and marked by circles; Figure 1B). The Pt single atoms on the surface of the Ni/C particles were further characterized by extended X-ray absorption fine structure (EXAFS) analysis in the R space (Figures 2A and S8; Table S1). The oscillation manners of the Pt L3-edge in the R space for the Pt_1Ni/C differ from those of the Pt foil. The Pt−Pt bond at 2.76 Å was not observed in Pt_1Ni/C. Compared to the Pt L3 edge of Pt foil probes by X-ray absorption near-edge spectroscopy (XANES) (Figure 2B), the adsorption edge for Pt_1Ni/C is ~11,570 eV, indicative of Pt(II) species. X-ray photoelectron spectroscopy (XPS) of Ni 2p and Pt 4f indicate that the majority of surface Ni and Pt species are in the 2+ oxidation state (Figure S2).[37]

The X-ray diffraction (XRD) profile of the Pt_1Ni/C catalyst shows a characteristic peak at 44° corresponding to (111) reflections of face-centered cubic Ni NPs (Figure S3), at the identical position observed in Ni/C, presumably as the low content of highly dispersed Pt does not influence the XRD pattern.

The H_2-temperature-programmed reaction (TPR) profiles (Figure 2C) indicate that alloying takes place in the Pt_1Ni/C catalyst. With the addition of single Pt atoms, the reduction temperature of Pt_1Ni/C (261°C) is shifted to lower regions compared with Ni/C (275°C). The adsorption of H_2 on the surface of the Pt_1Ni/C catalyst was investigated through H_2 temperature-programmed desorption (TPD) measurements (Figure 2D). The first peak (at 425°C) in the Pt_1Ni/C catalyst is at a much lower temperature than that observed for Ni/C (at 698°C), indicating that the Pt atoms provide low-barrier exit routes for H_2 during the desorption process.

Performance evaluation

The performance of the Pt_1Ni/C catalyst was investigated in the depolymerization of lignin using birch sawdust as the substrate. For comparison, single Pt atoms and Ni NPs supported on C (Pt_1/C and Ni/C) were prepared and applied in the same depolymerization reaction under identical conditions (Figure 3). The monomer yields are used as a measure of depolymerization efficiency of the catalysts. Under 5 MPa H_2 in methanol at 200°C, the yield of total monomers with the Pt_1Ni/C catalyst is 37% after 18 h (Figure 3, entry 1), quite close to the theoretical maximum monomer yield, which ranges from 44 to 56 wt%.[13] The yield of total monomers is significantly higher than that with the control catalysts (Figure 3, entries 2 and 3) and reported Ni/C, with monomer yields

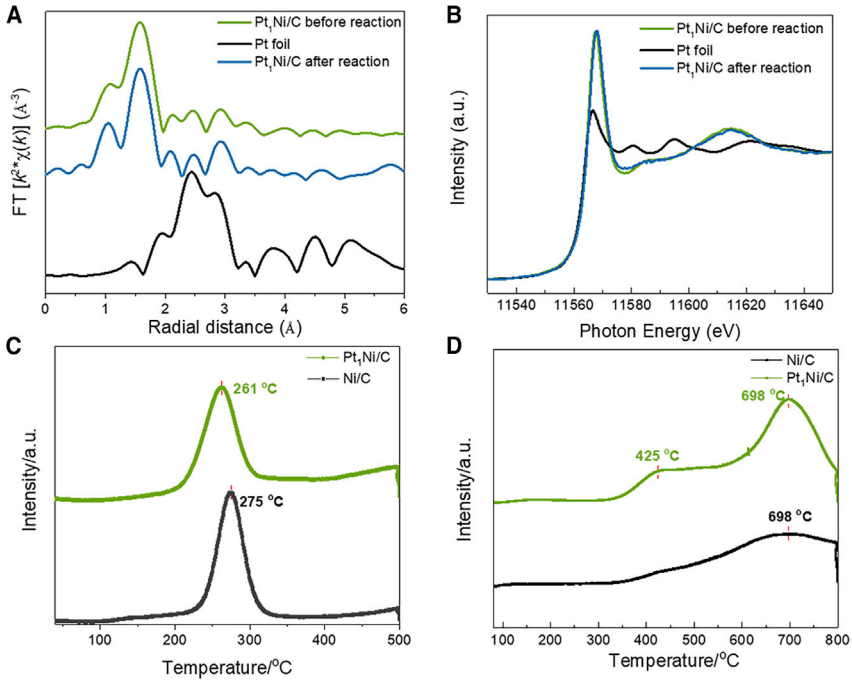

Figure 2. Characterizations of Pt_1Ni/C and Ni/C

(A) Pt L_3-edge EXAFS spectra in R space of Pt foil (control) and the Pt_1Ni/C catalyst before and after reaction. Pt foil was used as the reference (the Pt_1Ni/C sample after reaction was obtained under similar reaction conditions to those used for the conversion of birch sawdust, except in the absence of birch sawdust).

(B) Pt L_3-edge XANES profiles of Pt foil and the Pt_1Ni/C catalyst before and after reaction.

(C) H_2-temperature-programmed reaction (TPR) profiles of the Pt_1Ni/C catalyst.

(D) H_2-temperature-programmed desorption (TPD) profiles of the Pt_1Ni/C catalyst.

of 24% at 200°C in methanol.[38] Further analysis of the product distribution shows that a combined selectivity toward 4-n-propylsyringol (S) and 4-n-propylguaiacol (G) exceeds 90% within the monomer fractions, whereas 4-n-propanolguaiacol (G-OH) and 4-n-propanolsyringol (S-OH) accounts for <5% of the monomers (Figure 3, entry 1). Similar to other reported single-atom catalysts (i.e., Co_1/C,[39] $Ru_1/ZnO/C$,[40] and Pd_1/CNx[41]), the aromatic rings are preserved with the Pt_1Ni/C catalyst even under more forcing reaction conditions, unlike pure NP catalysts that lead to ring hydrogenation.[42,43] Saturated compounds were not observed with the Ni/C catalyst at 200°C, although traces of saturated compounds were detected at 300°C. It has been shown that Pt NPs are more active than Ni NPs in hydrogenolysis.[44] As the hydrogenolysis of C–O bonds is highly metal dependent,[45] the overall yield in S and G may be attributed to the high activity of Pt atoms. Note that in the absence of the metallic sites the monomer yield is very low (Figure 3, entry 4).

After separating the liquid products and drying the solid residue of birch sawdust and catalysts, 0.1 g birch sawdust was added to perform the recycling test. The decrease in the activation of the catalyst may be caused by coking on the surface of the catalyst (Table S2).

The mechanism of reductive fractionation involves solvolysis of the C–O bonds, with the catalyst hydrogenating the reactive intermediate products generated, preventing re-polymerization.[46,47] Based on the similar temperatures used, both Ni NPs and single Pt atoms contribute to H_2 dissociation (Figure 2C). Compared with Pt_1/C,

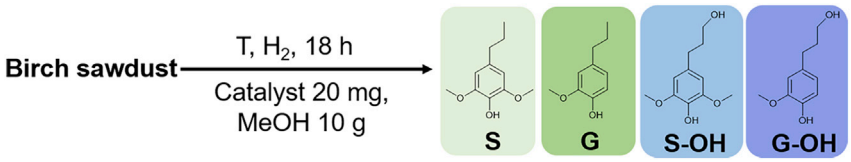

Figure 3. The monomer yield and main lignin-derived monomers obtained

	Catalyst	Total yield of monomers (%)	S (%)	G (%)	S-OH (%)	G-OH (%)
1	Pt_1Ni/C	37	23	12	0.1	0.5
2	Pt_1/C	14	3	2	5	2
3	Ni/C	24	9	6	5	3
4	C	6	1	–	–	–

Reaction conditions: 0.1 g birch sawdust, 0.02 g catalyst, 5 mL MeOH, 5 MPa H_2, 200°C, and 18 h.

which is less active with hydrogen dissociation, both Ni NPs and single Pt atoms in Pt_1Ni/C served as active sites in H_2 dissociation and adsorption of H atoms, so that a more abundant amount of H atoms can be produced on the surface of Pt_1Ni/C. Compared with Ni/C, the better performance of Pt_1Ni/C is due to the lower hydrogen binding energy of Pt atoms than Ni atoms. The H_2-TPD analysis shows a large decrease in the H_2 desorption temperature of the Pt_1Ni/C catalyst (425°C) (Figure 2D), compared with that of Ni/C (698°C), indicating that the single Pt atoms serve as active sites. Moreover, due to the single-atom nature of the Pt in the Pt_1Ni/C, the aromatic structure of the phenyl rings of lignin monomers are preserved without further hydrogenation. Since ring hydrogenation requires coordination of the aromatic ring over a trimetal face, NP catalysts would lead to the hydrogenation of aromatic rings,[42,43] while single Pt atoms can achieve hydrogenolysis of the C–O bonds without the hydrogenation of the phenyl ring.[48] As such, Pt single atoms played a pivotal role in Pt_1Ni/C in enhancing the catalytic activity while keeping the high selectivity in the lignin depolymerization, a benefit that cannot be achieved by using Ni/C only. Other reasons for the high activity, such as support effects, cannot be excluded.

The reaction conditions were optimized to obtain monophenolic compounds in higher yields (Figure 3). The yield of monophenolic compounds increased from 12 wt% at 150°C to 43 wt% at 300°C at a H_2 pressure of 5 MPa in methanol after 18 h (Figure 4A), with high selectivity to S and G (>90%, Figure 4B). At lower H_2 pressures (and in the absence of H_2), G-OH and S-OH are preferentially formed instead of G and S (Figure 4C).

A comparison of product distributions in water, methanol, ethanol, 1-propanol, 1-butanol, and ethylene glycol (Figure 4D) shows that solvent has a remarkable impact on the monomer yield as well as the product distribution, as observed elsewhere.[49,50] The solubility of lignin in different solvents has been extensively studied,[51] with the solubility in ethylene glycol being the highest followed by methanol, ethanol, 1-propanol, 1-butanol, and H_2O.[52] The monomer yields basically decrease with the decreasing solubility of lignin in the solvent. As in our case, a comparably lower yield of 32% in the pure ethylene glycol was obtained than that from methanol, probably due to the high viscosity and low solubility of H_2 in ethylene glycol.

DISCUSSION

We describe a selective hydrogenation catalyst in which monodispersed Pt atoms are anchored on the surface of Ni NPs supported on active carbon. The Pt_1Ni/C

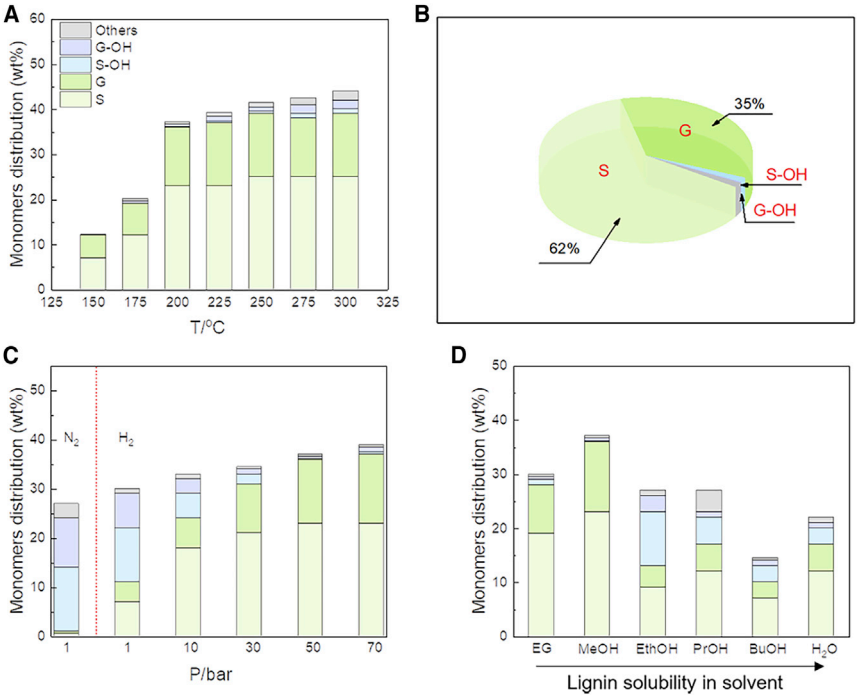

Figure 4. Effects of reaction conditions on the yields of lignin monomers

(A) Yields of lignin monomers obtained from birch sawdust as a function of temperature. Reaction conditions: 0.1 g birch sawdust, 0.02 g Pt_1Ni/C, 5 mL MeOH, 5 MPa H_2, 200°C, and 18 h.

(B) Monomer distribution at 200°C in MeOH. Reaction conditions are the same as those in (A).

(C) Yields of lignin monomers obtained from birch sawdust as a function of H_2 pressure. Reaction conditions: 0.1 g birch sawdust, 0.02 g Pt_1Ni/C, 5 mL MeOH, H_2, 200°C, and 18 h.

(D) Yields of lignin monomers obtained from birch sawdust in various solvents. Reaction conditions: 0.1 g birch sawdust, 0.02 g Pt_1Ni/C, 5 mL solvent, 5 MPa H_2, 200°C, and 18 h. BuOH, 1-butanol; EG, ethylene glycol; EthOH, ethanol; H_2O, water; MeOH, methanol; PrOH, 1-propanol.

catalyst affords monophenolic compounds in a 37 wt% yield at 200°C, which is close to the theoretical maximum yield. The remarkable activity and selectivity of the Pt_1Ni/C catalyst may be attributed to the synergistic effects between the Ni NPs and the single Pt atoms.

EXPERIMENTAL PROCEDURES

Synthesis of Ni/C

C powder (Vulcan XC 72R, 1 g) was mixed with 50 mL 5 M nitric acid at 80°C and stirred for 18 h. The solids were separated by centrifugation and were washed with distilled water until constant pH was achieved. The pre-treated activated carbon (200 mg) was dispersed in ethanol (20 mL) under vigorous stirring at room temperature. To the resulting suspension, a solution containing $Ni(NO_3)_2 \cdot 6H_2O$ (50 mg, 0.2 mmol) in ethanol (5 mL) was slowly added and stirring was continued for 12 h at room temperature. The reaction mixture was further heated at 40°C under stirring until all of the solvent had evaporated. The remaining solid was heated to 400°C for 1 h under H_2 in a tube furnace, to afford Ni/C.

Synthesis of Pt_1Ni/C

The Pt_1Ni/C catalyst was prepared via galvanic replacement between Ni NPs and $Pt(acac)_2$. Ni/C was dispersed in ethanol (50 mL), and the resulting suspension was heated at 50°C for 10 min. To the reaction mixture, a solution of $Pt(acac)_2$ (6 mg,

0.015 mmol) dissolved in toluene (5.2 mL) was added slowly. After stirring for 6 h at 50°C, the solution was cooled to room temperature. Then, the sample was collected by centrifugation and washed with ethanol (3 × 10 mL) and hexane (3 × 10 mL). After drying in vacuum at 40°C for 24 h, the Pt_1Ni/C catalyst was obtained as a black powder.

Synthesis of Pt_1/C

C powder (Vulcan XC 72R, 1 g) was mixed with 50 mL 5 M nitric acid at 80°C and stirred for 18 h. The solids were separated by centrifugation and were washed with distilled water until constant pH was achieved. This pre-treated activated carbon (100 mg) was dispersed in water (20 mL) under magnetic stirring. K_2PtCl_4 aqueous solution (10 mL, 0.043 mg/mL) was slowly added to the resulting reaction mixture. After stirring at room temperature for 30 min, the solid was collected by centrifugation. The isolated solid was washed with water (3× 10 mL) and dried at 60°C in vacuum for 24 h. The Pt_1/C was obtained as a black powder, and the HAADF-STEM images and elements mapping of Pt_1/C are in Figure S6.

XAFS analysis

Pt L3-edge XAFS data were recorded under fluorescence mode with a 32-element Ge solid-state detector at the SuperXAS beamline of Swiss Light Source (SLS) at the Paul Scherrer Institute (PSI, Villigen, Switzerland). The energy was calibrated according to the L3 absorption edge of pure Pt foil. Data analysis was performed using a standardized IFEFFIT package (including Athena and Artemis software).[53]

TEM, XPS, and XRD measurements

The Pt_1Ni/C powders were suspended in acetone and the resulting suspension was ultrasonicated for 1 h. Subsequently, the acetone suspension of NPs was deposited on a C film coated with Cu grid and then analyzed by TEM (FEI Talos, operated at 200 keV). XPS analysis were performed using a monochromatic Al Kα X-ray source of 24.8 W power with a beam size of 100 μm. XRD measurements were recorded in Bragg Brentano geometry on a Bruker D8 Discover diffractometer, equipped with a Lynx Eye XE detector, using non-monochromated Cu-Kα radiation.

Catalyst testing

In a typical reaction, birch sawdust (0.1 g, size 0.25–0.5 mm) and Pt1Ni/C (0.02 g) in MeOH (5 mL) were added into a 100-mL stainless-steel batch reactor with a glass liner. The reactor was sealed, flushed with H_2 3 times, and then pressurized to 5 MPa at room temperature. The reaction mixture was heated at 100°C for 3 h under stirring at 800 rpm, and then heated to 200°C. After 18 h, the autoclave was cooled in water and then depressurized.

Resource availability

Lead contact

Further information and requests for resources should be directed to and will be fulfilled by the lead contact, Paul Dyson (paul.dyson@epfl.ch).

Materials availability

All materials generated in this study are available from the lead contact without restriction.

Data and code availability

All data generated in this study can be found in the article and supplemental information or is available from the lead contact upon request.

SUPPLEMENTAL INFORMATION

Supplemental information can be found online at https://doi.org/10.1016/j.xcrp.2021.100567.

ACKNOWLEDGMENTS

The authors are grateful to the Swiss National Science Foundation and EPFL for financial support. L.P. acknowledges funding from the Swiss National Science Foundation under the Early Postdoc.Mobility Grant P2ELP2_195109. J.L. acknowledges funding from the European Union's Horizon 2020 Research and Innovation program under the Marie Skłodowska-Curie Grant agreement no. 838686. The authors thank Dr. Maarten Nachtegaal and Mr. Urs Vogelsang for technical support at the Super-XAS beamline of SLS.

AUTHOR CONTRIBUTIONS

All of the authors contributed to the design of the experiments and data analysis. L.C. performed the experiments, L.B. performed the HAADF-STEM tests, and J.L. performed the EXAFS measurements. L.C. and P.J.D. wrote the manuscript, and all of the authors discussed, commented on, and proofread the manuscript.

DECLARATION OF INTERESTS

The authors declare no competing interests.

Received: June 15, 2021
Revised: July 26, 2021
Accepted: August 16, 2021
Published: September 7, 2021

REFERENCES

1. Wong, S.S., Shu, R., Zhang, J., Liu, H., and Yan, N. (2020). Downstream processing of lignin derived feedstock into end products. Chem. Soc. Rev. *49*, 5510–5560.

2. Radhakrishnan, R., Patra, P., Das, M., and Ghosh, A. (2021). Recent advancements in the ionic liquid mediated lignin valorization for the production of renewable materials and value-added chemicals. Renew. Sustain. Energy Rev. *149*, 111368. https://doi.org/10.1016/j.rser.2021.111368.

3. Schutyser, W., Renders, T., Van den Bosch, S., Koelewijn, S.F., Beckham, G.T., and Sels, B.F. (2018). Chemicals from lignin: an interplay of lignocellulose fractionation, depolymerisation, and upgrading. Chem. Soc. Rev. *47*, 852–908.

4. Jing, Y., Dong, L., Guo, Y., Liu, X., and Wang, Y. (2020). Chemicals from Lignin: A Review of Catalytic Conversion Involving Hydrogen. ChemSusChem *13*, 4181–4198.

5. Jing, Y., Guo, Y., Xia, Q., Liu, X., and Wang, Y. (2019). Catalytic Production of Value-Added Chemicals and Liquid Fuels from Lignocellulosic Biomass. Chem *5*, 2520–2546.

6. Hu, J., Zhang, Q., and Lee, D.J. (2018). Kraft lignin biorefinery: a perspective. Bioresour. Technol. *247*, 1181–1183.

7. Gillet, S., Aguedo, M., Petitjean, L., Morais, A.R.C., Da Costa Lopes, A.M., Łukasik, R.M., and Anastas, P.T. (2017). Lignin transformations for high value applications: towards targeted modifications using green chemistry. Green Chem. *19*, 4200–4233.

8. Xu, C., Arancon, R.A.D., Labidi, J., and Luque, R. (2014). Lignin depolymerisation strategies: towards valuable chemicals and fuels. Chem. Soc. Rev. *43*, 7485–7500.

9. Parsell, T., Yohe, S., Degenstein, J., Jarrell, T., Klein, I., Gencer, E., Hewetson, B., Hurt, M., Kim, J.I., Choudhari, H., et al. (2015). A synergistic biorefinery based on catalytic conversion of lignin prior to cellulose starting from lignocellulosic biomass. Green Chem. *17*, 1492–1499.

10. Sun, Z., Fridrich, B., de Santi, A., Elangovan, S., and Barta, K. (2018). Bright Side of Lignin Depolymerization: Toward New Platform Chemicals. Chem. Rev. *118*, 614–678.

11. Upton, B.M., and Kasko, A.M. (2016). Strategies for the conversion of lignin to high-value polymeric materials: Review and perspective. Chem. Rev. *116*, 2275–2306.

12. Alonso, D.M., Wettstein, S.G., and Dumesic, J.A. (2012). Bimetallic catalysts for upgrading of biomass to fuels and chemicals. Chem. Soc. Rev. *41*, 8075–8098.

13. Yan, N., Zhao, C., Dyson, P.J., Wang, C., Liu, L.T., and Kou, Y. (2008). Selective degradation of wood lignin over noble-metal catalysts in a two-step process. ChemSusChem *1*, 626–629.

14. Van den Bosch, S., Schutyser, W., Koelewijn, S.-F., Renders, T., Courtin, C.M., and Sels, B.F. (2015). Tuning the lignin oil OH-content with Ru and Pd catalysts during lignin hydrogenolysis on birch wood. Chem. Commun. (Camb.) *51*, 13158–13161.

15. Ruppert, A.M., Weinberg, K., and Palkovits, R. (2012). Hydrogenolysis goes bio: from carbohydrates and sugar alcohols to platform chemicals. Angew. Chem. Int. Ed. Engl. *51*, 2564–2601.

16. Binder, J.B., and Raines, R.T. (2009). Simple chemical transformation of lignocellulosic biomass into furans for fuels and chemicals. J. Am. Chem. Soc. *131*, 1979–1985.

17. Liu, W., Chen, Y., Qi, H., Zhang, L., Yan, W., Liu, X., Yang, X., Miao, S., Wang, W., Liu, C., et al. (2018). A Durable Nickel Single-Atom Catalyst for Hydrogenation Reactions and Cellulose Valorization under Harsh Conditions. Angew. Chem. Int. Ed. Engl. *57*, 7071–7075.

18. Galkin, M.V., and Samec, J.S.M. (2014). Selective route to 2-propenyl aryls directly from wood by a tandem organosolv and palladium-catalysed transfer hydrogenolysis. ChemSusChem *7*, 2154–2158.

19. Kumaniaev, I., Subbotina, E., Sävmarker, J., Larhed, M., Galkin, M.V., and Samec, J.S.M. (2017). Lignin depolymerization to monophenolic compounds in a flow-through system. Green Chem. *19*, 5767–5771.

20. Huang, X., Zhu, J., Korányi, T.I., Boot, M.D., and Hensen, E.J.M. (2016). Effective Release of Lignin Fragments from Lignocellulose by Lewis Acid Metal Triflates in the Lignin-First Approach. ChemSusChem *9*, 3262–3267.

21. Albers, P., Pietsch, J., and Parker, S.F. (2001). Poisoning and deactivation of palladium catalysts. J. Mol. Catal. Chem. *173*, 275–286.

22. Liu, L., and Corma, A. (2018). Metal Catalysts for Heterogeneous Catalysis: From Single Atoms to Nanoclusters and Nanoparticles. Chem. Rev. *118*, 4981–5079.

23. Giannakakis, G., Flytzani-Stephanopoulos, M., and Sykes, E.C.H. (2019). Single-Atom Alloys as a Reductionist Approach to the Rational Design of Heterogeneous Catalysts. Acc. Chem. Res. *52*, 237–247.

24. Wang, A., Li, J., and Zhang, T. (2018). Heterogeneous single-atom catalysis. Nat. Rev. Chem. *2*, 65–81.

25. Sankar, M., Dimitratos, N., Miedziak, P.J., Wells, P.P., Kiely, C.J., and Hutchings, G.J. (2012). Designing bimetallic catalysts for a green and sustainable future. Chem. Soc. Rev. *41*, 8099–8139.

26. Pozzo, M., and Alfè, D. (2009). Hydrogen dissociation and diffusion on transition metal (= Ti, Zr, V, Fe, Ru, Co, Rh, Ni, Pd, Cu, Ag)-doped Mg(0001) surfaces. Int. J. Hydrogen Energy *34*, 1922–1930.

27. Kyriakou, G., Boucher, M.B., Jewell, A.D., Lewis, E.A., Lawton, T.J., Baber, A.E., Tierney, H.L., Flytzani-Stephanopoulos, M., and Sykes, E.C.H. (2012). Isolated metal atom geometries as a strategy for selective heterogeneous hydrogenations. Science *335*, 1209–1212.

28. Chen, Y., Ji, S., Chen, C., Peng, Q., Wang, D., and Li, Y. (2018). Single-Atom Catalysts: Synthetic Strategies and Electrochemical Applications. Joule *2*, 1242–1264.

29. Cui, X., Li, W., Ryabchuk, P., Junge, K., and Beller, M. (2018). Bridging homogeneous and heterogeneous catalysis by heterogeneous single-metal-site catalysts. Nat. Catal. *1*, 385–397.

30. Zhang, J., Liu, J., Xi, L., Yu, Y., Chen, N., Sun, S., Wang, W., Lange, K.M., and Zhang, B. (2018). Single-Atom Au/NiFe Layered Double Hydroxide Electrocatalyst: Probing the Origin of Activity for Oxygen Evolution Reaction. J. Am. Chem. Soc. *140*, 3876–3879.

31. Zhang, H., Liu, G., Shi, L., and Ye, J. (2018). Single-Atom Catalysts: Emerging Multifunctional Materials in Heterogeneous Catalysis. Adv. Energy Mater. *8*, 1701343.

32. Jiao, L., and Jiang, H.-L.L. (2019). Metal-Organic-Framework-Based Single-Atom Catalysts for Energy Applications. Chem *5*, 786–804.

33. Lu, Y., Wang, J., Yu, L., Kovarik, L., Zhang, X., Hoffman, A.S., Gallo, A., Bare, S.R., Sokaras, D., Kroll, T., et al. (2019). Identification of the active complex for CO oxidation over single-atom Ir-on-MgAl 2 O 4 catalysts. Nat. Catal. *2*, 149–156.

34. Tian, S., Wang, Z., Gong, W., Chen, W., Feng, Q., Xu, Q., Chen, C., Chen, C., Peng, Q., Gu, L., et al. (2018). Temperature-Controlled Selectivity of Hydrogenation and Hydrodeoxygenation in the Conversion of Biomass Molecule by the Ru_1/mpg-C_3N_4 Catalyst. J. Am. Chem. Soc. *140*, 11161–11164.

35. Zhou, J., An, W., Wang, Z., and Jia, X. (2019). Hydrodeoxygenation of phenol over Ni-based bimetallic single-atom surface alloys: mechanism, kinetics and descriptor. Catal. Sci. Technol. *9*, 4314–4326.

36. Park, S.J., and Seo, M.K. (2011). Interface Applications in Nanomaterials (Elsevier).

37. Antoniak, C., Gruner, M.E., Spasova, M., Trunova, A.V., Römer, F.M., Warland, A., Krumme, B., Fauth, K., Sun, S., Entel, P., et al. (2011). A guideline for atomistic design and understanding of ultrahard nanomagnets. Nat. Commun. *2*, 528.

38. Anderson, E.M., Katahira, R., Reed, M., Resch, M.G., Karp, E.M., Beckham, G.T., and Román-Leshkov, Y. (2016). Reductive Catalytic Fractionation of Corn Stover Lignin. ACS Sustain. Chem. Eng. *4*, 6940–6950.

39. Rautiainen, S., Di Francesco, D., Katea, S.N., Westin, G., Tungasmita, D.N., and Samec, J.S.M. (2019). Lignin Valorization by Cobalt-Catalyzed Fractionation of Lignocellulose to Yield Monophenolic Compounds. ChemSusChem *12*, 404–408.

40. Wang, S., Zhang, K., Li, H., Xiao, L.-P., and Song, G. (2021). Selective hydrogenolysis of catechyl lignin into propenylcatechol over an atomically dispersed ruthenium catalyst. Nat. Commun. *12*, 416.

41. Park, J., Cahyadi, H.S., Mushtaq, U., Verma, D., Han, D., Nam, K.-W., Kwak, S.K., and Kim, J. (2020). Highly Efficient Reductive Catalytic Fractionation of Lignocellulosic Biomass over Extremely Low-Loaded Pd Catalysts. ACS Catal. *10*, 12487–12506.

42. Bjelić, A., Grilc, M., Huš, M., and Likozar, B. (2019). Hydrogenation and hydrodeoxygenation of aromatic lignin monomers over Cu/C, Ni/C, Pd/C, Pt/C, Rh/C and Ru/C catalysts: mechanisms, reaction micro-kinetic modelling and quantitative structure-activity relationships. Chem. Eng. J. *359*, 305–320.

43. Huš, M., Bjelić, A., Grilc, M., and Likozar, B. (2018). First-principles mechanistic study of ring hydrogenation and deoxygenation reactions of eugenol over Ru(0001) catalysts. J. Catal. *358*, 8–18.

44. Sergeev, A.G., and Hartwig, J.F. (2011). Selective, nickel-catalyzed hydrogenolysis of aryl ethers. Science *332*, 439–443.

45. Zakzeski, J., Bruijnincx, P.C.A., Jongerius, A.L., and Weckhuysen, B.M. (2010). The catalytic valorization of lignin for the production of renewable chemicals. Chem. Rev. *110*, 3552–3599.

46. Van Den Bosch, S., Renders, T., Kennis, S., Koelewijn, S.F., Van Den Bossche, G., Vangeel, T., Deneyer, A., Depuydt, D., Courtin, C.M., Thevelein, J.M., et al. (2017). Integrating lignin valorization and bio-ethanol production: on the role of Ni-Al2O3catalyst pellets during lignin-first fractionation. Green Chem. *19*, 3313–3326.

47. Anderson, E.M., Stone, M.L., Katahira, R., Reed, M., Beckham, G.T., and Román-Leshkov, Y. (2017). Flowthrough Reductive Catalytic Fractionation of Biomass. Joule *1*, 613–622.

48. Zhang, B., Asakura, H., Zhang, J., Zhang, J., De, S., and Yan, N. (2016). Stabilizing a Platinum 1 Single-Atom Catalyst on Supported Phosphomolybdic Acid without Compromising Hydrogenation Activity. Angew. Chem. *128*, 8459–8463.

49. Balogh, D.T., Curvelo, A.A.S., and De Groote, R.A.M.C. (1992). Solvent Effects on Organosolv Lignin from Pinus caribaea hondurensis. Holzforschung *46*, 343–348.

50. Schutyser, W., Van Den Bosch, S., Renders, T., De Boe, T., Koelewijn, S.-F.F., Dewaele, A., Ennaert, T., Verkinderen, O., Goderis, B., Courtin, C.M., et al. (2015). Influence of bio-based solvents on the catalytic reductive fractionation of birch wood. Green Chem. *17*, 5035–5045.

51. Song, Q., Wang, F., Cai, J., Wang, Y., Zhang, J., Yu, W., and Xu, J. (2013). Lignin depolymerization (LDP) in alcohol over nickel-based catalysts via a fragmentation–hydrogenolysis process. Energy Environ. Sci. *6*, 994.

52. Yu, O., Yoo, C.G., Kim, C.S., and Kim, K.H. (2019). Understanding the Effects of Ethylene Glycol-Assisted Biomass Fractionation Parameters on Lignin Characteristics Using a Full Factorial Design and Computational Modeling. ACS Omega *4*, 16103–16110.

53. Ravel, B., and Newville, M. (2005). ATHENA, ARTEMIS, HEPHAESTUS: data analysis for X-ray absorption spectroscopy using IFEFFIT. J. Synchrotron Radiat. *12*, 537–541.